Fractional vortices in the XY model with π bonds

R. V. Kulkarni*[1,2], E. Almaas[1], K. D. Fisher[1], and D. Stroud[1]
[1] *Department of Physics, The Ohio State University, Columbus, Ohio 43210*
[2] *Department of Physics, University of California at Davis, Davis, California 95616*
(February 23, 2009)

We define a new set of excitations in the XY model which we call "fractional vortices". In the frustrated XY model containing π bonds, we make the ansatz that the ground state configurations can be characterized by pairs of oppositely charged fractional vortices. For a chain of π bonds, the ground state energy and the phase configurations calculated on the basis of this ansatz agree well with the results from direct numerical simulations. Finally, we discuss the possible connection of these results to some recent experiments by Kirtley *et al* [Phys. Rev. B **51**, R12057 (1995)] on high-T_c superconductors where fractional flux trapping was observed along certain grain boundaries.

PACS numbers: 75.10.Hk, 0.50.+q, 74.72.-h, 74.50.+r

I. INTRODUCTION

The classical XY Hamiltonian is one of the most studied models in statistical physics. In its usual, unfrustrated form, it is written

$$H = \sum_{\langle ij \rangle} J_{ij}[1 - \cos(\phi_i - \phi_j)], \tag{1}$$

where ϕ_i is a phase variable on the i^{th} site ($0 \leq \phi < 2\pi$), the sum runs over distinct pairs $\langle ij \rangle$, and J_{ij} is the energy of the coupling between sites i and j. In the ferromagnetic, nearest-neighbor case, J_{ij} vanishes except between nearest-neighbor sites and all the J_{ij}'s are equal to a single positive constant J. In this case, for spatial dimensionality $d \geq 3$, there is a phase transition to a ferromagnetic state at a critical temperature, with conventional critical phenomena. If $d = 2$, there is instead the Kosterlitz-Thouless-Berezinskii phase transition, in which pairs of oppositely charged integer vortices unbind at a finite temperature T_{KTB}[1]. The classical XY model has been found to describe a wide variety of systems with complex scalar order parameters, including bulk superconductors in $d = 3$, superconducting films, Josephson junction arrays in $d = 2$, and superfluid He_4 films[2].

Recently, the XY model with *anti ferromagnetic* bonds i.e, with bond strengths $J_{ij} < 0$ (also called π *bonds*), has received much attention[3–9], in particular due to its possible relevance to high-T_c superconductors and other experimental systems[10–12]. Specifically, if we consider the grain boundary between two high-T_c superconductors with suitable misorientation of the crystalline axes, then the resulting Josephson coupling across the boundary can have the coupling energy $J_{ij} < 0$[7]. This is a consequence of the $d_{x^2-y^2}$ symmetry of the order parameter in many high-T_c materials. Such grain-boundary interfaces have lately been studied in a variety of experiments and in several geometries. These experiments have led to interesting results, such as the observation of the trapping of half-integer and also other fractional flux quanta[13–15]. These results can be explained using models involving π bonds[9,16–20]. Similar models involving π bonds have also been developed to explain such phenomena as the paramagnetic Meissner effect[8], also observed in samples of high-T_c superconductors.

A key concept in understanding the effects of π bonds is "frustration." Consider, for example, the XY model on a square lattice with only the nearest-neighbor couplings nonvanishing. If a plaquette has an odd number of bonds, that plaquette is frustrated, in the sense that no choice of angles in the four grains making up the plaquette can simultaneously minimize *all* the bond energies. Thus, a single π bond will cause the two plaquettes adjoining that π bond to become frustrated. In a *line* of π bonds, only the two plaquettes at the end of the line will become frustrated. Because of the frustrated plaquettes, it is non-trivial to find the ground state of the XY-model with π bonds. In this paper, we will show, both numerically and by analytical arguments, that these ground states are characterized by certain spatial phase configurations which we call fractional vortices. We will also derive an expression for the interaction energy of two fractional vortices in the XY model.

The rest of the paper is organized as follows. In Section II, we define the fractional vortices and calculate the interaction energy of a bound pair of fractional vortices for the XY model. In Section III, we study the ground state of XY-lattices containing a single π bond, two π bonds, and a string of π bonds. In each case, using a variational ansatz for the ground-state configuration, we find that there is a critical π bond strength, above which the ground state contains pairs of oppositely charged fractional vortices. To check these results, we directly calculate the ground-state energy of these lattices using a numerical relaxation technique based on the equations of motion for overdamped Josephson junctions. We find that both the ground-state energy and the critical π bond

strength, predicted by the variational approach, are in excellent agreement with the numerical results. Finally, in Section IV, we discuss the possible relevance of these numerical results to experiments carried out in systems containing π junctions, such as high-T_c superconductors containing grain boundaries and tricrystals, as recently studied by Kirtley *et al*[13–15].

II. FRACTIONAL VORTICES IN THE UNFRUSTRATED XY MODEL

Consider the Hamiltonian (1) for an XY model defined on a square lattice with $N \times N$ sites. If all the nearest-neighbor couplings are equal, this may be written

$$H = J \sum_{\langle ij \rangle} [1 - \cos(\phi_i - \phi_j)]. \tag{2}$$

Hereafter, we shall use units such that $J = 1$. The phase angle, ϕ_i, at point (x_i, y_i) due to a fractional vortex of charge q at point (x_0, y_0) is *defined* to be

$$\phi_i(x_0, y_0, q) = q \times \tan^{-1}(\frac{y_i - y_0}{x_i - x_0}). \tag{3}$$

For $q = 1$, we recover the standard configuration for an integer vortex. This definition can be seen as a generalization of the concept of half-vortices introduced by Villain[21] for the same model. Note that, while for the integer vortex the bond angles change continuously, the fractional vortex case is characterized by a branch cut, across which the bond angles are discontinuous.

This singularity leads to several other distinctions between integer and fractional vortices. For example, the energy associated with a single integer vortex is proportional to $\ln(N)$. In the thermodynamic limit, this is a weak divergence which makes the KTB vortex-antivortex unbinding transition possible. By contrast, the energy of an unbound fractional vortex is $\propto N$, since the number of bonds along the branch cut is $\propto N$. Thus, it is energetically unfavorable at all temperatures to create isolated fractional vortices. But a bound pair of fractional vortices with charges q and $-q$ is much less expensive energetically, because then the branch cut is restricted to the line joining the two charges: the total energy should be proportional to the separation of the fractional vortices. For fixed q and large enough separations, this energy is always larger than that of a pair of oppositely charged *integer* vortices, whose energy varies as the logarithm of their separation. Nevertheless, for fixed separation, it is always possible to find a non-integer q such that that the energy of the fractional vortex pair is less than the corresponding energy for the integer vortices. In the following, we derive expressions for the energy of a bound pair of fractional vortices in the XY model, and compare them to numerical results obtained by calculating the energy explicitly for these configurations.

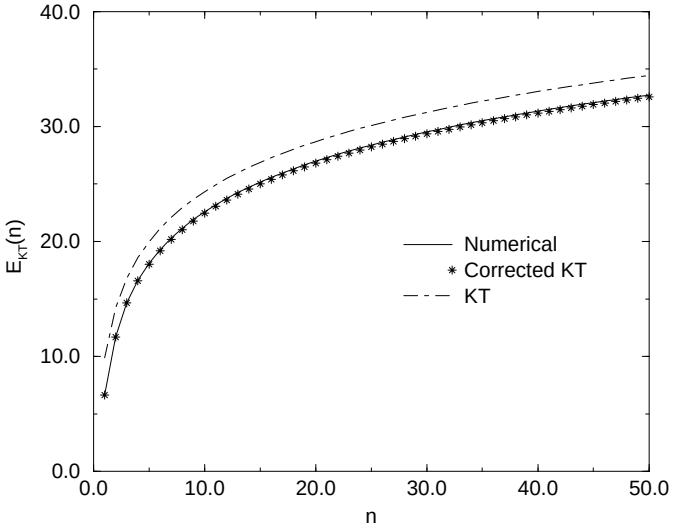

FIG. 1. Calculated energy of a bound pair of integer vortices as a function of separation n, in units of J. Full curve: numerically exact results. Dot-dashed curve: KT-approximation [Eq. (5)]. Asterisks: KT-approximation plus core correction.

We first consider a bound pair of integer vortices of charge ± 1 located at (x_0, y_0) and (x_1, y_1). The standard KT expression for the energy of the pair is obtained by approximating the Hamiltonian as

$$H \sim \frac{1}{2} \sum_{<ij>} (\phi_i - \phi_j)^2. \tag{4}$$

For the phase configuration, we use $\phi_i = \phi_i(x_0, y_0, +1) + \phi_i(x_1, y_1, -1)$, where $x_1 - x_0 = n$ and $y_1 - y_0 = 0$ (in units of the lattice constant a). Substituting this configuration into (4) gives the Kosterlitz-Thouless formula for the interaction energy, E_{KT}, of two oppositely charged integer vortices:

$$E_{KT}(n) = 2\pi \left[\ln n + \frac{\pi}{2} \right]. \tag{5}$$

In Fig. 1, we compare this expression to the energy of a pair of oppositely charged integer vortices, computed using the same phase configuration but the exact H. The discrepancy arises from the expansion of the cosine factor, which is inaccurate for the bonds closest to the vortices. This inaccuracy is remedied by a making a core correction i.e, by calculating the contribution from the bonds on the perimeter of the plaquettes surrounding the vortices exactly, rather than by a quadratic expansion. For large n, the core-correction energy, $E_c(n)$, is approximately given by

$$E_c(n) = \pi^2 - 8 + \frac{12 - \pi^2}{2n^2} + \frac{8 + \pi^2}{16n^4}. \tag{6}$$

As can be seen from Fig. 1, the numerically calculated energy is well approximated by $E_{KT}(n) + E_c(n)$.

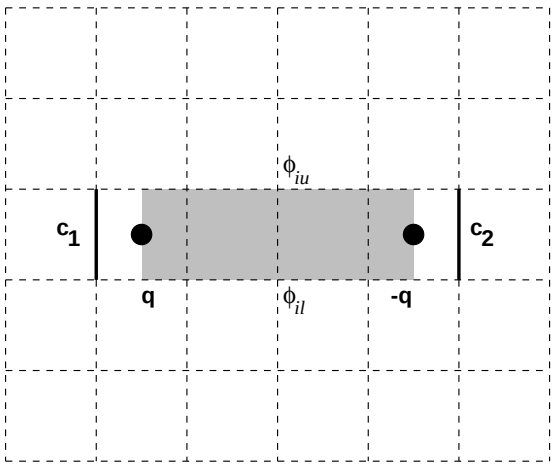

FIG. 2. Schematic drawing of a bound pair of fractional vortices arranged parallel to the x-axis. For this configuration, the vortices are separated by three plaquettes. ϕ_{iu} and ϕ_{il} are the phases at the two ends of bonds in the shaded region (region A); the angle $\theta_{i,A}$ in the text is defined by $\theta_{i,A} \equiv \phi_{iu} - \phi_{il}$. Core corrections are calculated only for the bonds denoted C_1 and C_2, as discussed in the text.

Next, we calculate the energy $E(q,n)$ of a pair of fractional vortices $\pm q$, separated by a distance n in the x-direction, as shown schematically in Fig. 2. Note that $E(1,n)$ is simply the interaction energy of a pair of integer vortices, as just discussed. The phase configuration of this pair is then given by $\phi_i = \phi_i(x_0, y_0, q) + \phi_i(x_1, y_1, -q)$, where $x_1 - x_0 = n$ and $y_1 - y_0 = 0$. We now divide the bonds into two groups: (A) those intersected by the line segment joining the two vortex centers; and (B) the remaining bonds. Let $E_A(q,n)$ and $E_B(q,n)$ be the corresponding energy contributions to $E(q,n)$ coming from these two groups of bonds. Thus $E(q,n) = E_A(q,n) + E_B(q,n)$. To obtain $E(q,n)$ we proceed as follows:

(1). We calculate $E_A(1,n)$, using the quadratic expansion for the cosine. $E_A(1,n)$ is simply the contribution to the total energy of a bound pair of integer vortices arising from the bonds along the branch cut. Note that there are n bonds in region A. Once $E_A(1,n)$ is known, we get $E_B(1,n) = E_{KT}(n) - E_A(1,n)$.

(2). We obtain $E_B(q,n)$ by noting that, in the quadratic approximation, $E_B(q,n) = q^2 E_B(1,n)$.

(3). Finally, we determine $E_A(q,n)$ by directly evaluating it using the full expression for the cosine, not the quadratic expansion. This is necessary, because the bond angles in region A are not small for arbitrary q.

We now use the outlined procedure to obtain $E(q,n)$.

Step 1: Let $\theta_{i,A}(1,n) \equiv \phi_{iu} - \phi_{il}$ denote the i^{th} *bond* angle (cf. Fig. 2) in region A for q = 1. For the two-vortex configuration, $\theta_{i,A}(1,n)$ is given by

$$\theta_{i,A}(1,n) = 2\left[\tan^{-1}\left(\frac{1}{2i-1}\right) + \tan^{-1}\left(\frac{1}{2n-2i+1}\right)\right] \quad (7)$$

Using the quadratic approximation, the corresponding energy contribution $E_A(1,n)$ is given by

$$E_A(1,n) = \frac{1}{2}\sum_{i=1}^{n} \theta_{i,A}^2(1,n). \quad (8)$$

Using the approximation: $\tan^{-1}[1/(2i-1)] \sim 1/(2i-1)$ for $i \geq 2$, we find

$$E_A(1,n) = \frac{\pi^2}{2} + \left(\frac{\pi}{2} + \frac{2}{2n-1}\right)^2 + \frac{2}{n}\left[\gamma + 2\ln 2 - 2 - 2n\right] + \frac{2}{n}\psi\left(n - \frac{1}{2}\right) - \psi'\left(n - \frac{1}{2}\right)$$
$$E_B(1,n) = E_{KT}(n) - E_A(1,n), \quad (9)$$

where $\psi(x)$ and $\psi'(x)$ are the Digamma function and its derivative, γ is Euler's constant, and E_{KT}(n) is given by Eq. (5).

Step 2. Using the results of step 1 and Eq. (5), we get

$$E_B(q,n) = q^2\left[2\pi \ln n + \pi^2 - E_A(1,n)\right]. \quad (10)$$

Step 3. The next step is to calculate $E_A(q,n)$. Bond angles in region A are given by

$$\theta_{i,A}(q,n) = q\left[2\pi - \theta_{i,A}(1,n)\right]. \quad (11)$$

Correspondingly, the energy $E_A(q,n)$ is given by

$$E_A(q,n) = \sum_{i=1}^{n}(1 - \cos\left[\theta_{i,A}(q,n)\right]). \quad (12)$$

Since the bond angle $\theta_{i,A}(q,n)$ is not small for an arbitrary q, we cannot expand the cosine term only to second order. But for *any* q, the difference $\theta_{i,A}(q,n) - \theta_{n/2,A}(q,n)$ *is* a small parameter for any $i \geq 2$. Expanding the cosine term in Eq. (12) to second order in this parameter, we obtain an expression for $E_A(q,n)$. This expression can be summed, and eventually gives

$$E_A(q,n) = (n-2)\left[(1 - \cos\alpha_n) + \frac{8q^2}{n^2}\cos\alpha_n + \frac{4q}{n}\sin\alpha_n\right]$$
$$+2\left\{1 - \cos\left[q\left(\frac{3\pi}{2} - \frac{2}{2n-1}\right)\right]\right\} - \left[\frac{4q^2}{n}\cos\alpha_n + q\sin\alpha_n\right]$$
$$\times \sum_{m=2}^{n-1}\theta_{m,A}(1,n) + \frac{q^2}{2}\cos\alpha_n \sum_{m=2}^{n-1}\theta_{m,A}^2(1,n), \quad (13)$$

where

$$\sum_{m=2}^{n-1}\theta_{m,A}(1,n) = 2\gamma - 4 + 4\ln 2 + 2\psi\left(n - \frac{1}{2}\right), \quad (14)$$

$$\sum_{m=2}^{n-1}\theta_{m,A}^2(1,n) = \pi^2 + \frac{4}{n}\left(\gamma + 2\ln 2 - 2 - 2n\right) + \frac{4}{n}\psi\left(n - \frac{1}{2}\right) - 2\psi'\left(n - \frac{1}{2}\right) \quad (15)$$

$$\alpha_n = q\left(2\pi - \frac{4}{n}\right). \quad (16)$$

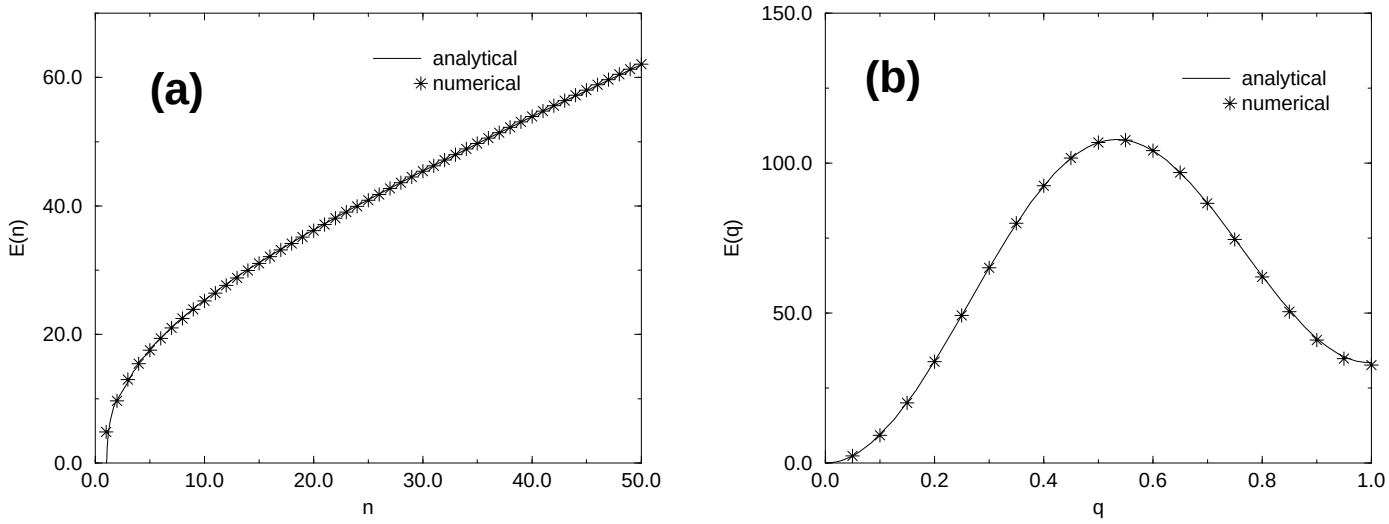

FIG. 3. Energy of a bound pair of fractional vortices in an unfrustrated XY-lattice as obtained numerically ($*$) and from the analytical approximation, Eq. (17) (full line), for (a) fixed charge, $q = 0.8$, as a function of separation; and (b) fixed separation, $n = 50$, as a function of charge.

Adding up the contribution from the two regions, we finally get the required expression for the energy of a bound pair of fractional vortices. As noted earlier, the core corrections must be included to attain high numerical accuracy. In the present case, it is sufficient to include these corrections only for the bonds labeled C_1 and C_2 in Fig. 2, using the procedure outlined earlier. This approximation is equivalent to extending region A to include bonds C_1 and C_2 . Correspondingly, the core-corrected total energy is given by

$$E(q,n) = E_A(q,n) + E_B(q,n) - q^2\theta_c^2 + 2\,[1-\cos(q\theta_c)] \tag{17}$$

where

$$\theta_c \;=\; \frac{\pi}{2} - \frac{2}{2n+1}. \tag{18}$$

Expressions (17) and (18) are compared to the results of numerical computation in Figs. 3(a) and 3(b); agreement between the two is excellent. On the basis of this agreement, which is equally good for all values of q and n which we have considered, we present this result as a good analytical expression for the interaction energy between two fractional vortices in the unfrustrated XY model on a square lattice. This result is a generalization of the integer vortex excitations proposed by Kosterlitz and Thouless.

For large n, we can further simplify the above expression by dropping terms of $\mathcal{O}(1/n)$ and smaller in Eq. (17) to get

$$E(q,n) = (n-2)[1-\cos(2\pi q)] + 2\ln n\left[\pi q^2 - q\sin(2\pi q)\right] + \frac{3}{4}\pi^2 q^2 \;+\; 2\left[1-\cos(\frac{3\pi q}{2})\right]. \tag{19}$$

III. FRACTIONAL VORTICES IN THE XY MODEL WITH π BONDS

The fractional vortex configurations introduced in the previous section provide a natural way of characterizing the ground state of the XY model containing π bonds. In this section, we implement this description by making a variational guess for the ground-state configuration using fractional vortices. We then compare our variational results with those obtained by numerically relaxing to the ground-state configuration, and find excellent agreement. In the following subsections, we will focus on obtaining the critical bond strength, λ_c, above which the ferromagnetic ground-state solution becomes unstable, and the ground-state configuration contains bound pairs of fractional vortices. For the case of one and two π bonds, we also compare our results to those from previous studies by Vannimenus *et al*[3]. Note that in these calculations, in which the goal is to calculate the threshold bond strength above which the ferromagnetic ground state becomes unstable rather than the absolute energies as a function of λ, it is unnecessary to include the core corrections. Hence, λ_c can be calculated analytically as demonstrated below. The ground-state configuration and energy for $\lambda > \lambda_c$ do need the core corrections for greatest accuracy. We obtain them numerically using our variational guess and discuss them in the subsequent section.

A. One π bond

We first consider the case of a single π bond i.e, a single antiferromagnetic bond in a host of ferromagnetic bonds.

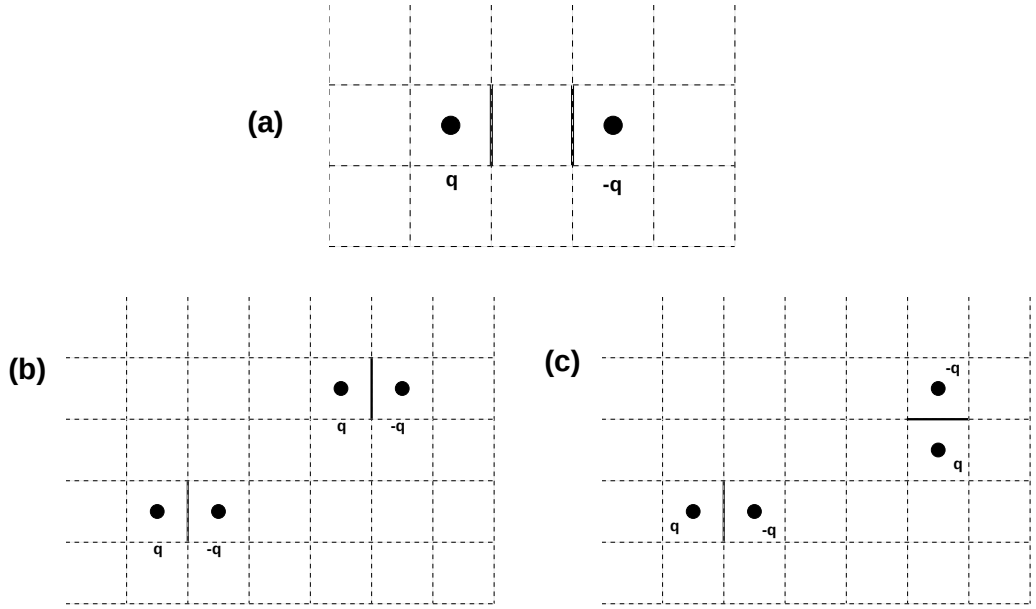

FIG. 4. Schematic plot of three configurations, each containing π bonds (full lines), which are (a) parallel and adjacent, (b) parallel and non-adjacent, and (c) perpendicular and non-adjacent. Also shown are the corresponding locations of the fractional vortex charges for the variational configurations.

As before, we take the bond strength of the ferromagnetic bonds to equal unity, and we denoted the strength of the antiferromagnetic bond by λ ($\lambda \geq 0$). The problem is to obtain the ground-state configuration and energy for arbitrary strength, λ, of the π bond.

To solve this problem, we make a variational guess for the ground-state configuration: it is the phase configuration corresponding to a bound pair of fractional vortices of strength $\pm q$, located at the centers of the two plaquettes adjacent to the π bond. The charge, q, is a variational parameter with respect to which the ground-state energy is minimized for a given λ.

The total energy of this configuration discussed above is readily obtained using the procedure of the previous section, suitably corrected for the fact that we have a π bond instead of a ferromagnetic bond. The angle difference across the π bond is given by $\theta_\pi = q\pi$. Then, using Eqs. (8) and (10), we get

$$E_B(q) = \frac{1}{2} q^2 \pi^2, \tag{20}$$

while from Eq. (12) we find

$$E_A(q) = 1 + \lambda \cos(q\pi). \tag{21}$$

Adding these two terms gives the total energy of the configuration. Minimizing this energy with respect to q yields the condition

$$q\pi = \lambda \ \sin(q\pi). \tag{22}$$

For $\lambda \leq 1$, the ground-state configuration corresponds to $q = 0$: all the phases are perfectly aligned. For $\lambda > 1$, the ground-state configuration corresponds to a bound pair of fractional vortices with charges $\pm q$ obtained by solving Eq. (22). Thus, the ferromagnetic ground state is unstable above a critical bond-strength value $\lambda_c = 1$. The same value has been obtained previously by workers using different approaches[3,4].

B. Two π bonds

We now consider the case of two parallel, adjacent π bonds. As before, our variational guess for the ground state is the configuration corresponding to a bound pair of fractional vortices; we take these to be located as shown in Fig. 4(a). The corresponding total energy is again calculated using the procedure outlined in Section II. Using Eqs. (8) and (10), the energy contribution $E_B(q)$ is

$$E_B(q) = q^2 \left\{ 2\pi \ln 2 + \pi^2 - \left[\frac{\pi}{2} + 2 \tan^{-1}(1/3) \right]^2 \right\}. \tag{23}$$

Using Eq. (12), we get

$$E_A(q) = 2 + 2\lambda \cos\left\{ 2q \left[3\pi/4 - \tan^{-1}(1/3) \right] \right\}. \tag{24}$$

Adding these two contributions gives the total energy, which is to be minimized with respect to q for a given λ. This procedure gives the critical value $\lambda_c = 0.563$, which is in good agreement with the exact value $\lambda_c = \pi/2 - 1$, obtained by Vannimenus *et al*[3].

Next, we consider the case of two parallel, but non-adjacent π bonds, as shown in Fig. 4(b). Taking the bond centers to have the coordinates $(0, 0)$ and (m, n),

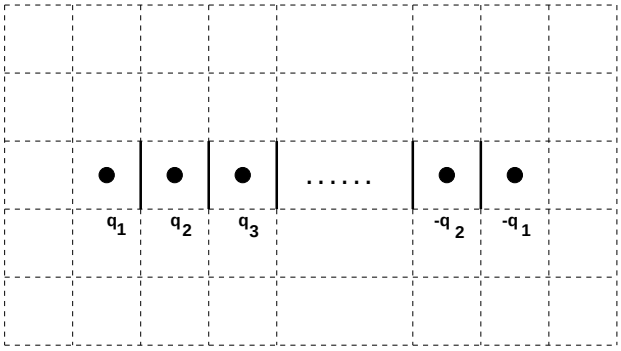

FIG. 5. Schematic plot of the assumed variational configuration containing m pairs of fractional charges, for a chain of π bonds (solid line segments) of length $2m$.

we calculate the energy using the variational procedure described above with vortex charges as shown. For large separation between the bonds ($\sqrt{m^2+n^2} \gg 1$), this procedure gives

$$E_B(q) = q^2 \left[2\pi^2 - 2\alpha_{mn} - (\pi - \alpha_{mn})^2\right] \tag{25}$$

and

$$E_A(q) = 2 + 2\lambda \cos\left[q(\pi + \alpha_{mn})\right], \tag{26}$$

where

$$\alpha_{mn} = \frac{m^2 - n^2}{(m^2+n^2)^2}. \tag{27}$$

Minimizing the total energy gives the critical bond strength as

$$\lambda_c = \frac{1 - 2\alpha_{mn}/\pi}{1 + 2\alpha_{mn}/\pi}. \tag{28}$$

Similarly, for two non-adjacent *perpendicular* π bonds [Fig. 4(c)], we find

$$E_B(q) = q^2 \left[2\pi^2 - 2\beta_{mn} - (\pi - \beta_{mn})^2\right] \tag{29}$$

and

$$E_A(q) = 2 + 2\lambda \cos\left[q(\pi + \beta_{mn})\right], \tag{30}$$

where

$$\beta_{mn} = \frac{2mn}{(m^2+n^2)^2}. \tag{31}$$

In this case, the critical bond strength is

$$\lambda_c = \frac{1 - \beta_{mn}/\pi}{1 + \beta_{mn}/\pi}. \tag{32}$$

These results are identical to those obtained previously by Vannimenus *et al*, using a different approach[3]. The agreement lends support to our hypothesis that the ground-state configuration of such systems can be characterized by a set of fractional vortices (in the cases considered here, a set of only two oppositely charged fractional vortices). Besides having the merit of simplicity, our approach also easily yields the ground-state configuration and energy for arbitrary λ. Moreover, our procedure can be used to obtain the ground-state even when the separation between the bonds is not large. In particular, for two parallel bonds such that $m = n = 1$, our variational procedure yields the surprising result that $\lambda_c = 1$ for this configuration. The same result was obtained in a numerical study done by Gawiec *et al*[5]. Finally, our variational ansatz can readily be generalized to longer π bond chains, as we shall see in the next section.

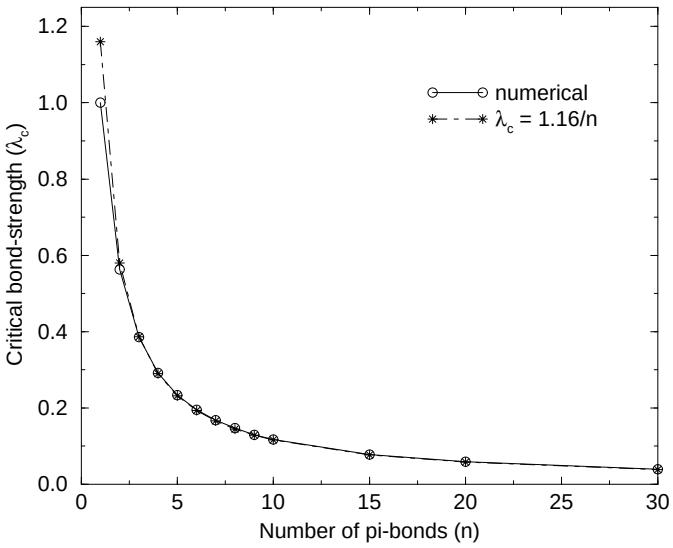

FIG. 6. Critical bond strength λ_c as function of chain length, for a chain of π bonds of length n. Open circles and full curve: numerical results. Asterisks and dashed curve: analytical approximation, $\lambda_c = \frac{1.16}{n}$.

C. Chains of π bonds

Next, we consider chains of π bonds of length $n \geq 3$. In this case, we make the variational ansatz that the ground state consists of $n/2$ or $(n+1)/2$ pairs of oppositely charged fractional vortices for even or odd n, arranged as shown in Fig. 5. As before, we proceed by calculating the contribution to the total energy from regions A and B. However, the procedure outlined in Section II has to be generalized to include many pairs of fractional vortices. Since the details are significantly different from that outlined in section II, we briefly describe the generalized procedure below.

(1). We consider the case in which all charges have magnitude unity. The total energy of this configuration is given simply by the KT expression

$$E_{KT} = -2\pi \sum_{j<k} q_j q_k \ln(n_{jk}) + \pi^2 \sum_j q_j^2, \tag{33}$$

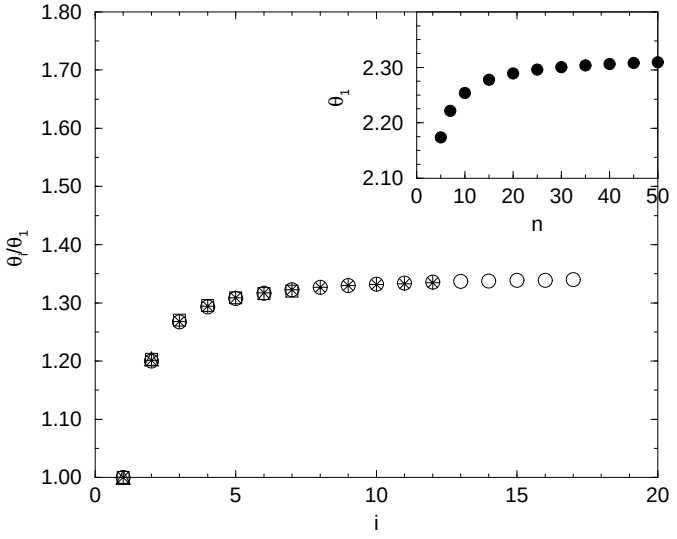

FIG. 7. Ratio of i^{th} bond angle, θ_i, to the first bond angle θ_1, plotted as a function of i for chain lengths $n = 5(\triangle), 15(\square), 25(*), 35(\circ)$. The bond strength is $\lambda = 1$. Inset: variation of θ_1 with chain length n, for $\lambda = 1$.

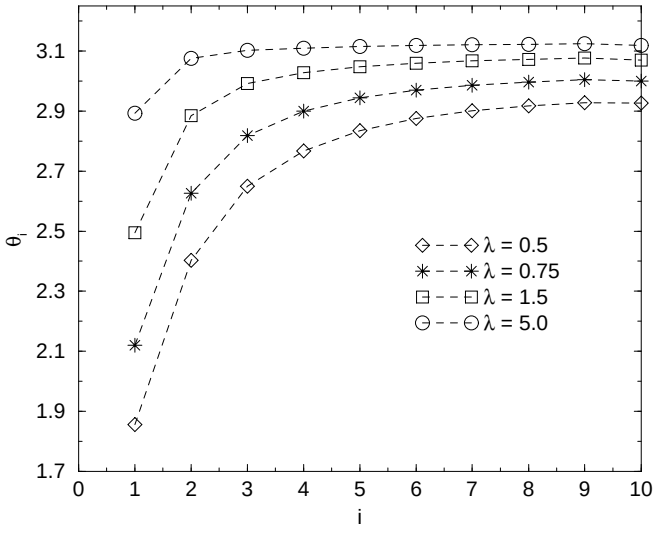

FIG. 8. The i^{th} bond angle, θ_i, plotted as a function of i for bond strengths $\lambda = 0.5, 1.0, 1.5, 2.0$. The chain length, n, is taken to be 20.

where n_{jk} is the distance between the charges q_j and q_k, and the second sum runs over all the individual charges, each of which has magnitude unity. This result is obtained by using a small-angle expansion for the contribution from each bond angle difference θ_b, and summing those contributions to give

$$E_{KT} = \frac{1}{2}\sum_b (\theta_b)^2. \tag{34}$$

The bond angle θ_b is, in turn, decomposed as

$$\theta_b = \sum_k q_k \theta_{k,b}, \tag{35}$$

where k labels the position of the charges and $\theta_{k,b}$ is the contribution to θ_b from a charge of unit magnitude at k.

(2). Next, we consider the case in which the charges are fractional ($|q| < 1$). The bonds can still be divided into classes A and B as discussed earlier. In the case of fractional charges, the bond angle differences in region B are still given by Eq. (35). Correspondingly, the energy contribution from bonds in region B is

$$\begin{aligned} E_B &= \frac{1}{2}\sum_b^B \theta_b^2 \\ &= \frac{1}{2}\sum_b^{A+B} \theta_b^2 - \sum_b^A \theta_b^2, \end{aligned} \tag{36}$$

where $\sum_b^B$ and $\sum_b^A$ denote sums over all bonds in region B and in region A.

(3). Finally we calculate the energy E_A, using suitable expressions for the bond angles in region A, as obtained from the multi-vortex configuration but without making the small angle expansion.

To minimize the resulting total energy, which is a function of all the q_k's, we used two procedures: (i) Powell's multidimensional direction set method[22], and (ii) a genetic algorithm[23]. Both methods successfully converged to the same minimum energy and configuration, from which we deduced the critical bond strength, λ_c, for various values of n. Fig. 6 shows our results for $\lambda_c(n)$. As can be seen from the main part of the figure, it fits very well to the approximate expression $\lambda_c \approx 1.16/n$. A consequence of this $1/n$ dependence is: if the system has a finite concentration of π bonds randomly distributed in the lattice, then in the thermodynamic limit $\lambda_c \to 0$. This behavior follows from the fact that, in the thermodynamic limit, there is always a finite probability of having an arbitrarily large chain length n, and hence an arbitrarily small λ_c.

We now look at the variations in the bond angles along the π bond chain as a function of chain length, n, and bond strength, λ (for $\lambda > \lambda_c$). First, we discuss the variation with fixed bond strength, taking $\lambda = 1$. Fig. 7 shows the ratio of the bond angles, θ_i, along the chain (not including the central bond) to the bond angle across the first π bond, θ_1, as a function of position along the chain for various chain lengths. A number of features deserve mention. First, for a chain of length $n = 2m$, the ratio of the bond angles, θ_i/θ_1, for $i < m$ is independent of m. Second, since the bond angle distribution is symmetric, we only need to look at the bonds in the range $1 \le i \le m$. Third, the bond angles increase monotonically as one moves along the chain from its edges to

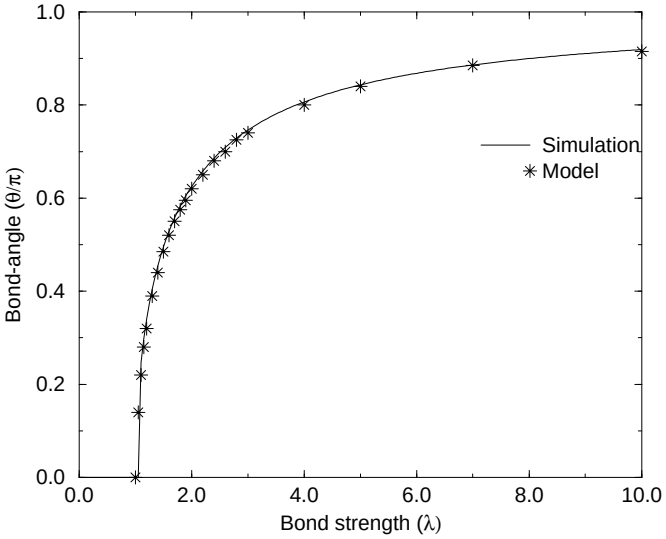

FIG. 9. Bond angle, θ, as function of bond strength λ for a single π bond obtained using (a) fractional-charge variational ansatz ($*$), and (b) numerical simulations (solid line).

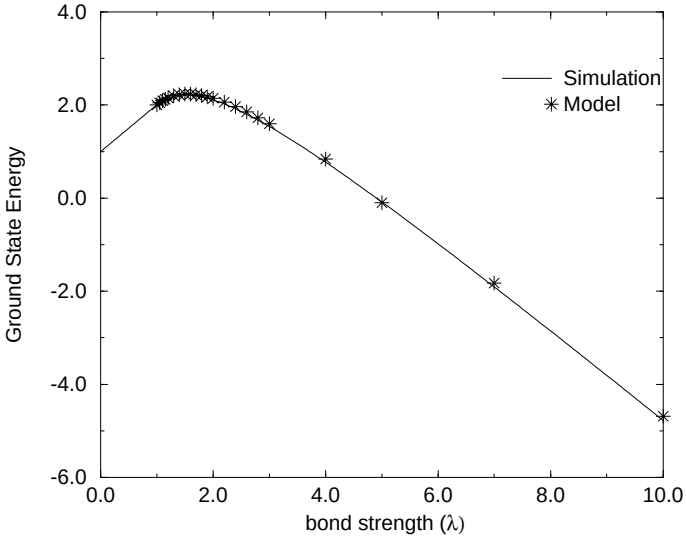

FIG. 10. Total energy as function of λ for a single π bond obtained using (a) variational ansatz ($*$), and (b) numerical simulations (solid line).

the center i.e, as i increases from 1 to m. The inset shows the variation of θ_1 with chain length for $\lambda = 1$. Note that with this choice of λ, the bond angles saturate quickly: they are roughly constant over the "interior bonds," such that $i \geq 3$. Furthermore, this constant value (approximated by the central bond angle) approaches π as the chain length n increases.

Fig. 8 shows how the bond angles, θ_i, vary with bond strength, λ, for a fixed chain length ($n = 20$). As already seen in the previous figure, θ_i rapidly tends to saturate towards its central value with increasing i. Moreover, the central bond angle quickly increases from 0 to π as λ increases for $\lambda > \lambda_c$. Thus, we can 'tune' the central bond angle to any desired fraction of π by appropriately adjusting λ.

Although the underlying variables are the θ_i's, it is of interest to mention corresponding trends in the fractional charges. For small λ, these charges decrease monotonically with increasing i, so that the largest charges reside at the ends of the chain. For larger λ, charges comparable in magnitude to those at the ends appear away from the ends.

D. Numerical Check of Variational Procedure.

To check our variational approach, we have carried out an independent minimization to calculate the ground-state energy of the system containing π bonds[24], *without* making any assumptions about the presence or absence of fractional vortices. To carry out this minimization, we imagine that the ij^{th} bond is actually an overdamped Josephson junction connecting nodes i and j. The current flowing through that bond from node i to node j is then

$$I_{ij} = I_{c,ij} \sin\left(\phi_i - \phi_j\right) + \frac{\hbar}{2eR_{ij}} \frac{d}{dt}\left(\theta_i - \theta_j\right), \qquad (37)$$

and the sum of these currents must equal the total external current, I_i^{ext}, fed into node i:

$$\sum_b I_{ij} = I_i^{ext}. \qquad (38)$$

where $I_{c,ij}$ is the critical current of the junction between grains i and j, and R_{ij} is the corresponding shunt resistance. These equations can be put into dimensionless form using the definitions $i_{ij} \equiv I_{ij}/I_c$ and $g_{ij} \equiv R/R_{ij}$, where I_c and R are a convenient normalizing critical current and shunt resistance, and introducing the natural time unit $\tau \equiv \hbar/(2eRI_c)$. Combining these equations yields a set of coupled ordinary differential equations which is easily reduced to matrix form and solved numerically, as described by many previous investigators[25]. For our work, we employed a fourth-fifth order Runge-Kutta integration with variable time step.

For present purposes, we are interested, not in examining the dynamical properties of arrays with π bonds, but rather in finding the minimum-energy configuration of such arrays. To that end, we have simply iterated this set of coupled equations of motion, with *no* external current, allowing the phases to evolve until they reach a time-independent configuration. As has been shown by previous workers, this configuration will correspond to a local minimum-energy state of the corresponding Hamiltonian $H = -\sum_{\langle ij \rangle} (\hbar I_{c;ij}/2e) \cos(\phi_i - \phi_j)$. We then compare the resulting configuration and energy with those predicted by the fractional vortex variational ansatz for the ground state.

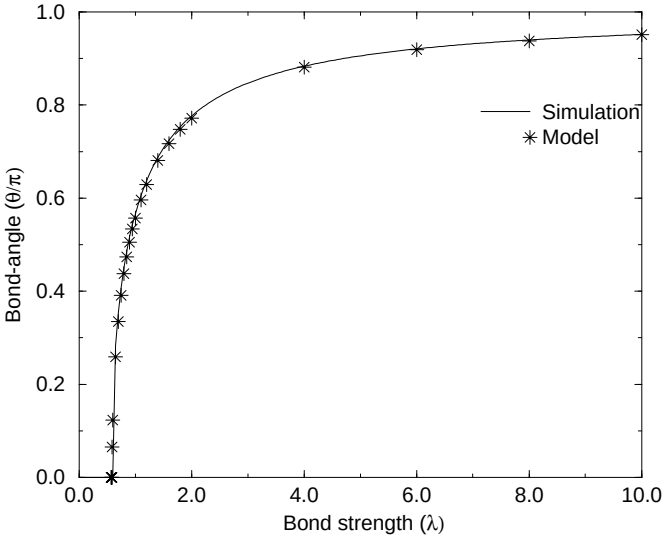

FIG. 11. Same as Fig. 9 but for two adjacent π bonds.

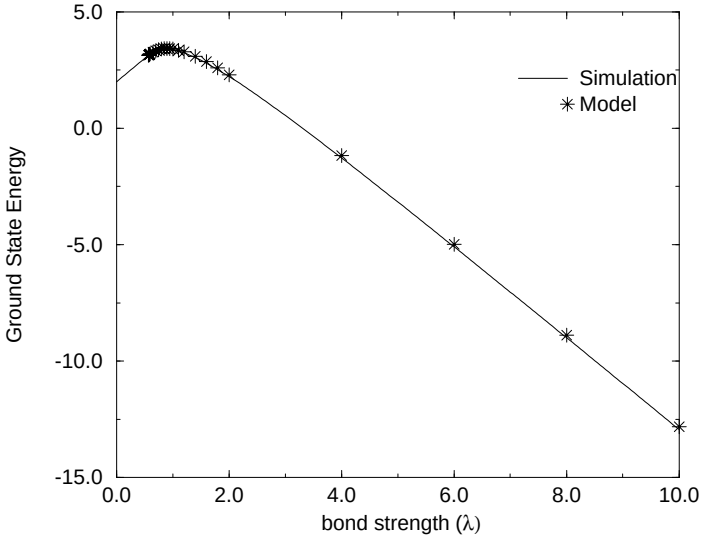

FIG. 12. Same as Fig. 10 but for two adjacent π bonds.

To make the comparison as straightforward as possible, we made the simplifying assumption $R_{ij} = R$ for all Josephson junctions, whether 0 or π. We took $i_{c,ij} = 1$ for all normal junctions, and $i_{c;ij} = -\lambda$ for all π junctions. Since no external current is to be applied to the system, we carry out these calculations using square arrays of junctions with periodic boundary conditions in both directions.

Each simulation begins with phases randomized at each grain. The system is then relaxed according to the Eqs. (37) and (38) for an interval of $50 - 100\tau$. We then evaluate the final energy, as well as the phase difference, θ_{ij}, across each π junction. Once equilibrium is reached for a given λ, we increment or decrement λ, and the system is allowed to relax again without re-randomizing the phases. Even quite large arrays (50×50 plaquettes) relax quite quickly using this procedure, except near the critical point, but care must be taken to avoid taking data from simulations in which the system is trapped in a metastable state. We have used arrays ranging from 10×10 plaquettes to 50×50, and occasionally as large as 70×70 to examine convergence of equilibrium values.

Figs. 9 and 10 show the the exact ground-state energy and corresponding q for the case of a single π bond in a host of normal bonds, as calculated by this numerical procedure. The results are also compared to the total energy obtained from a ground-state configuration corresponding to a pair of bound fractional vortices of charge $\pm q$, calculated numerically. As shown in the figures, the agreement is excellent, thereby indicating that the ground-state energy is indeed well characterized by a bound pair of fractional vortices.

Figs. 11 and 12 show a similar comparison for the case of two π bonds. Once again, the results obtained numerically from the RSJ equations for both the total energy and the bond angle across the π bonds, are in excellent agreement with those found from the fractional vortex ansatz, suggesting that the ground state, in the case of two π bonds, is again well characterized, over a range of λ, by a pair of oppositely charged fractional vortices.

Finally, we briefly discuss the accuracy of our variational approximation for the "wave function," i. e., the phase distribution in the ground state. As is well known, a variational wave function may give an excellent value for the ground state energy, but a less accurate picture of the ground state configuration. In particular, our variational approach ignores the spin-wave degrees of freedom in characterising the ground state of the frustrated XY model, but it is possible that they may be required to get an accurate description of the phase distribution. To test the accuracy of our variational phase distribution, we have compared it to the exact (numerical) phase distribution in the ground state in several cases. The difference between the two configurations is shown graphically in Fig. 13 for the case of two π bonds. As can be seen, the difference between the variational and exact wave functions is almost always less than 2-3% of the bond angle at the π junction. We have looked at the results for one and two π bonds for varying bond strengths, and in all cases considered the discrepancy is small. Thus, we conclude that the phase distribution as well as the energy is well approximated by our variational ground state involving only fractional vortices.

IV. SUMMARY AND POSSIBLE SIGNIFICANCE

The original motivation for this work was to study π bonds in relation to the experiments of Kirtley *et al*[13–15] on π-*grain boundaries* in high-T_c superconductors.

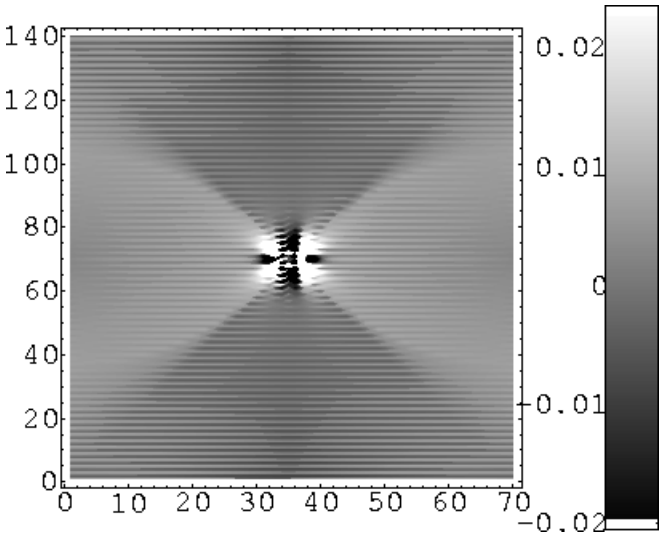

FIG. 13. Graphical representation of the difference between the variational phase configuration (two oppositely charged fractional vortices) and the numerically obtained ground state phase configuration for the case: $\lambda = 10$, $N_\pi = 2$ (string of two adjacent parallel π bonds). The phase difference, as a fraction of the bond angle across the π junctions, is shown on a gray scale given at the right edge of the diagram. A 70x70 lattice is considered and alternate stripes along the y-axis represent vertical and horizontal bonds. The π bond string is shown in center of the Figure.

Sigrist and Rice[6] have shown that the Josephson coupling across a grain boundary between two d-wave superconductors can have either sign, depending on their crystallographic orientations, thereby giving rise to the possibility of π-grain boundaries. Of course, in the present model, we are treating not a π-grain boundary, but rather a string of π bonds in the discrete XY model. Nevertheless, we argue that this string could be viewed as a crude model of such a grain boundary. It has been argued that even so-called 'single-crystal' high-T_c superconductors can be effectively represented as an array of superconducting grains weakly interacting via the Josephson coupling between them[26]. The typical lattice spacing for the high-T_c materials in such a model has been quoted to be as large as 1 μm. Thus, the chain of π bonds in our model can be taken as representing the coupling of grains across a π-grain boundary, and the length of the chain will depend on the dimensions of the grain boundary, and the interpretation of the effective lattice spacing.

Now we turn to a summary of the experiments. The relevant experiments fall into two categories. In the tricrystal experiments, the intersections of three grain boundaries at a "tricrystal point" were studied[14,15]. At special orientations of the grain boundaries, these experiments found that a half quantum of flux is trapped around the tricrystal point - a result that has been interpreted as verifying the d-wave symmetry of the superconducting order parameter. In the tricrystal geometry, observing a trapped half-flux quantum can then be explained by the fact that one of the grain boundaries can be taken to be a π-boundary[9,17]. In the second class of experiments, a triangular (or a hexagonal) single-crystal superconductor was inserted into a single crystal superconducting host of the same material, but with crystal axes misoriented with respect to those of the inclusion. In these systems, Kirtley *et al*[13] have found evidence of *fractional* (not half-integer) flux entrapment. These results have been interpreted[27] as evidence that the superconducting order parameter violates time-reversal symmetry, either in the bulk or at an interface. Indeed, recent experiments have reported fractional flux entrapment even in the absence of π-grain boundaries[28], possibly supporting the existence of an order parameter which violates time-reversal symmetry.

If, in the triangular inclusion, only one of the three boundaries is a π-boundary, the two "zero" boundaries will have little effect on the arrangement of the order parameter phases, and can reasonably be ignored. Similarly, in the tricrystal, if only one of the three grain boundaries is a π-boundary, this boundary would correspond to a semi-infinite chain of π bonds, while the other two "zero" boundaries can again be ignored in the model. Thus, a finite chain of π bonds may be suitable for modeling the triangular inclusions, and the extrapolation for long chain lengths is relevant for the tricrystal experiments.

Next, we speculate about the relationship of our results to the observed trapping of non-half-integers of flux in triangular inclusions. The trapped flux is usually related to the phase difference across the grain boundary by the following argument[7], which we restate to apply to our geometry. Consider a closed integration contour C (of radius $r \gg a$) centered at one end of the grain boundary, and passing through the grain boundary. We wish to consider the flux enclosed by this loop. The path is taken to be deep inside the grains, so that the Meissner effect dictates that the supercurrent density $\mathbf{j} = 0$. Since $\mathbf{j} \propto \nabla\phi - (2\pi/\Phi_0)\mathbf{A}$, where ϕ is the phase of the superconducting wave function, $\Phi_0 = hc/(2e)$ is the superconducting flux quantum, and $\mathbf{A}$ is the vector potential, it follows that

$$\nabla\phi = \frac{2\pi}{\Phi_0}\mathbf{A}. \tag{39}$$

Now let $C = C^1 + C^2$, where C^1 is the part of the contour not including the grain boundary. In the approximation that C^2 can be taken to be infinitesimally short, the integral $\int_{C^2} \mathbf{A}\cdot\mathbf{d}\ell \sim 0$. In addition, we have $\int_{C^2} \nabla\phi\cdot\mathbf{d}\ell = \Delta\phi$, the phase discontinuity across the grain boundary. But also ϕ must be continuous around C, modulo 2π. Combining all these conditions with Eq. (39), we find that

$$\Delta\phi = 2\pi n - \frac{2\pi}{\Phi_0}\Phi, \tag{40}$$

where n is an integer and Φ is the flux enclosed by the *entire* contour. Thus, the flux enclosed by C is related

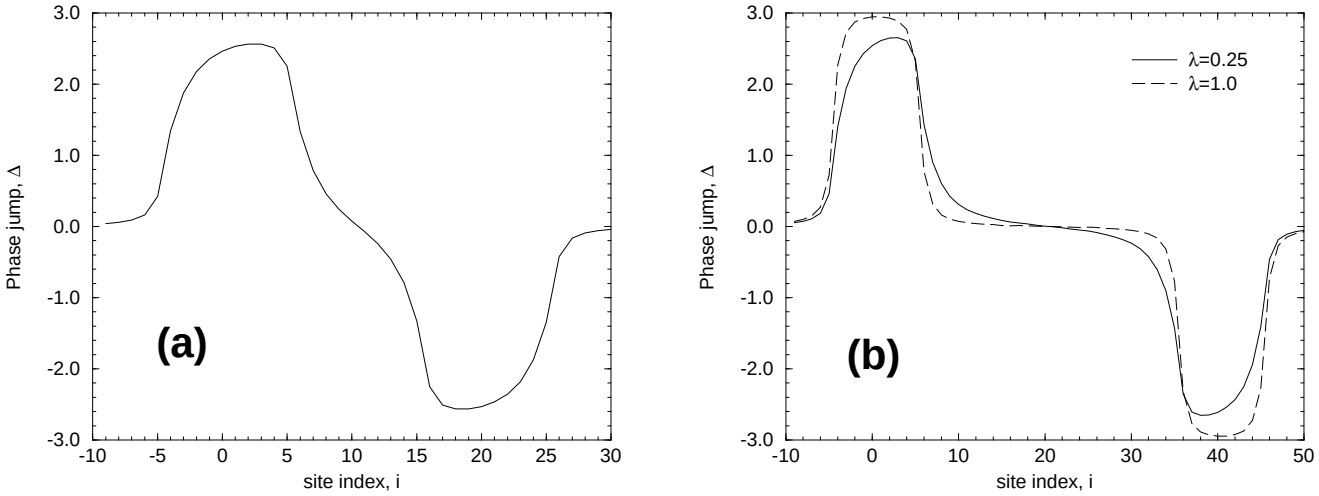

FIG. 14. The calculated phase jump, Δ, which corresponds to the flux measured by a SQUID of size 10×10 lattice spacings, for a chain of π bonds of length n and bond strength λ. The x coordinate denotes the position of the center of the SQUID relative to the leftmost π bond. Δ is defined to be the sum, taken in the counterclockwise direction, of the phase discontinuities across those bonds intersected by the perimeter of the SQUID, which are either π bonds in the grain boundary, or lie along the extension of the grain boundary along the $\pm x$ direction. (a) $n = 20$, $\lambda = 0.25$. (b) $n = 40$, $\lambda = 0.25$ (full curve) and 1.0 (dashed curve).

to the *phase defect* across the π junction in the loop. In particular, if $\Delta\phi$ is a *non-half-integer fraction* of 2π in the ground state, then the flux enclosed will also correspondingly be fractional. Hence, a non-half-integer fractional flux is correlated with a phase jump across the grain boundary which is a non-integer fraction of π.

Our results show that $\Delta\phi \neq \pi$ for an interior bond in a finite chain of π bonds. In fact $\Delta\phi$ can be 'tuned' to be any fraction of π by simply varying the strength of the bonds for any finite chain length. Thus, a necessary condition for the occurrence of a non-half-integer flux quantum is indeed satisfied. But this result still does not demonstrate that the the trapped vortices correspond to non-half-integer flux quanta, because our calculations do not include the magnetic fields induced by the currents near the π-grain boundary. These fields will change $\mathbf{A}$, and hence, the phase arrangement itself to some extent. Thus, we cannot rigorously infer the magnetic flux when these inductive effects are omitted from the calculations[29].

Although our present calculations do not include these inductive effects, it is still instructive to look at the phase distribution as if Eq. (40) were valid anyway. In particular, let us try to model the flux configuration obtained by scanning the π-grain boundary using an idealized square SQUID. We take the flux through the SQUID to be the same as that through the corresponding contour C as described above. According to the argument just given, the flux passing through the SQUID is therefore proportional to the sum of the phase jumps $\Delta = \sum_i \Delta\phi_i$ around the SQUID contour, across those bonds for which the phase has a discontinuity. In our simplified model for the flux through the SQUID, these discontinuities occur across the two bonds where the contour, taken counterclockwise around the SQUID, intersects the π-grain boundary or its extension along the x axis.

In order to make a reasonable connection to the experimental geometry, we estimate the lattice spacing a in our model using

$$E_J = I_c \Phi_0 / c = a^2 J_c \Phi_0 / c, \tag{41}$$

where E_J is the Josephson coupling energy between adjacent grains, I_c is the associated intergranular critical current, J_c is the macroscopic critical current density set by the Josephson effect coupling, and a is the lattice spacing of the granular array.

Using the experimental estimates for E_J and J_c (see Ref. 13), we estimate $a = 1.1\mu m$, which is in agreement with the typical value for these materials[26]. Since the triangular insertions are roughly $20\mu m$ in length (for each side), we have looked at the results for a π bond chain of length 20 lattice spacings, with the SQUID diameter also taken to correspond to the experimental diameter. In Fig. 14(a), we show Δ as calculated for a π bond chain of length $n = 20$ and strength $\lambda = 0.25$, and a SQUID of diameter $d = 10$. In Fig. 14(b), we show the same for a chain of length $n = 40$. We note that for a fixed bond strength, Δ becomes more concentrated near the chain ends with increasing chain length n. Furthermore, we can also make Δ more localized near the chain ends by increasing λ, as shown in Fig. 14(b).

The profile of Δ, shown in Fig. 14(a), strikingly resembles the *flux profile* measured in Ref. 13 across one side of a triangular insertion. In view of this similarity,

it would be interesting to see if the changes we see with bond strength and chain length are also found experimentally. (Experimentally, the strength of the bonds can be changed by varying the misorientation angles of the inclusions.) If inductive effects do not change the qualitative picture presented above, then these experiments would provide evidence supporting the interpretation of the grain boundary as a string of π bonds.

We also comment on the fact that Kirtley *et al*[13] were able to reproduce their measured flux configuration with a certain arrangement of fractional magnetic charges. Our picture suggests one way of understanding *why* this modeling works. The key is that the flux distribution is closely related to the *gauge-invariant* phase jump ($\Delta\gamma_{ij}$) across the boundary, given by

$$\Delta\gamma_{ij} = \Delta\phi_{ij} - (2\pi/\Phi_0)\Delta A_{ij}, \tag{42}$$

where i, j label sites connected by a bond across the grain boundary, and ΔA_{ij} and $\Delta\phi_{ij}$ are the corresponding discontinuities in the vector potential and the phase across that bond. A nonzero $\Delta\gamma_{ij}$ can therefore be attributed either to a nonzero $\Delta\phi_{ij}$ or a nonzero ΔA_{ij} (or a combination of both). In our calculations, we have assumed a nonzero $\Delta\phi_{ij}$ and take $\Delta A_{ij} = 0$ across the branch cut. The opposite choice ($\Delta A_{ij} \neq 0$, $\Delta\phi_{ij} = 0$) corresponds to a fractional magnetic monopole, since the vector potential of a magnetic monopole changes discontinuously across a branch cut[30]. Since the physical quantity is the gauge-invariant phase difference, these pictures are equivalent.

In summary, we have introduced a set of "fractional vortex " excitations in the XY model, and have derived an expression for the interaction energy of a bound pair of fractional vortices. Furthermore, we have studied the ground state of the XY model on a two-dimensional lattice containing π bonds. For strings of π bonds of any length, we find that there exists a minimum bond strength, above which the ground state can be characterized by pair(s) of oppositely charged fractional vortices. We have verified this ansatz by carrying out independent numerical simulations for the ground-state configuration of this system. Finally, we have discussed the possible connection between these calculations and the trapped fractional flux quanta, which are observed near grain boundaries in high-T_c superconductors.

V. ACKNOWLEDGMENTS

We would like to thank Kathryn Moler, Yong-Baek Kim and Rajiv Singh for helpful conversations. We are grateful for support from NSF grant DMR97-31511, the Midwest Superconductivity Consortium through Purdue University. Grant No. DE-FG 02-90 45427, and NASA, Division of Microgravity Sciences, Grant No. NCC 8-152. RVK would also like to acknowledge the support of the US Department of Energy, Office of Science, Division of Materials Research. Calculations were carried out using the IBM SP2 and the ORIGIN 2000 at the Ohio Supercomputer Center.

---

* Electronic address: kulkarni@rilke.ucdavis.edu

[1] J. M. Kosterlitz, and D. J. Thouless, J. Phys. C **6**, 1181 (1973).
[2] D. R. Nelson in *Phase Transitions and Critical Phenomena*, edited by C. Domb and J. L. Lebowitz (Academic Press, New York, 1983) and references therein.
[3] J. Vannimenus, S. Kirkpatrick, F. D. M. Haldane, and C. Jayaprakash, Phys. Rev. B **39**, 4634 (1989).
[4] G. N. Parker, and W. M. Saslow, Phys. Rev. B **38**, 11718 (1988).
[5] P. Gawiec, and D. R. Grempel, Phys. Rev. B **44**, 2613 (1991).
[6] M. Sigrist, and T. M. Rice, J. Phys. Soc. Jpn. **61**, 4283 (1992).
[7] M. Sigrist, and T. M. Rice, Rev. Mod. Phys. **67**, 503 (1995).
[8] D. Dominguez, E. A. Jagla, and C. A. Balseiro, Phys. Rev. Lett. **72**, 2773 (1994).
[9] D. B. Bailey, M. Sigrist, and R. B. Laughlin, Phys. Rev. B **55**, 15239 (1997).
[10] D. Sieger, H. Tietze, R. Geick, P. Schweiss, W. Treutmann, and P. Frings, Solid State Commun. **64**, 1413 (1987).
[11] K. Katsumata, J. Tuchendler, Y. J. Uemura, and H. Yoshizawa, Phys. Rev. B **37**, 356 (1988).
[12] S. Higgins, and R. A. Cowley, J. Phys. C **21**, 2215 (1988).
[13] J. R. Kirtley, P. Chaudhari, M. B. Ketchen, N. Khare, S.-Y. Lin, and T. Shaw, Phys. Rev. B **51**, R12057 (1995).
[14] J. R. Kirtley, C. C. Tsuei, J. Z. Sun, C. C. Chi, L. S. Yu-Jahnes, A. Gupta, M. Rupp, and M. B. Kitchen, Nature **373**, 225 (1995).
[15] C. C. Tsuei, J. R. Kirtley, C. C. Chi, L. S. Yu-Jahnes, A. Gupta, T. Shaw, J. Z. Sun, and M. B. Ketchen, Phys. Rev. Lett. **73**, 593 (1994).
[16] A. J. Millis, Phys. Rev. B **49**, R15408 (1994).
[17] V. B. Geshkenbein, A. I. Larkin, and A. Barone, Phys. Rev. B **36**, 235 (1987).
[18] M. Sigrist, and Y. B. Kim, J. Phys. Soc. Jpn. **63**, 4314 (1994).
[19] R. G. Mints, and V. G. Kogan, Phys. Rev. B **55**, R8682 (1997)
[20] J. R. Kirtley, K. A. Moler, and D. J. Scalapino, Phys. Rev. B **56**, 886 (1997).
[21] J. Villain, J. Phys. C **10**, 1717 (1977); **10**, 4793 (1977).
[22] W. H. Press, S. A. Teukolsky, W. T. Vetterling, and B. P. Flannery, *Numerical Recipes* (Cambridge University Press, 1992).
[23] M. Mitchell, *An introduction to genetic algorithms* (MIT Press, Cambridge Mass., 1996) and references therein.
[24] K. D. Fisher, Ph.D. thesis 1999, The Ohio State University.
[25] See, for example, Wenbin Yu, K. H. Lee, and D. Stroud, Phys. Rev. B **47**, 5906 (1993) and references cited therein.

[26] M. Tinkham, *Introduction to Superconductivity* (McGraw-Hill, New York, 1996); M. Tinkham and C.J. Lobb in *Solid State Physics*, edited by H. Ehrenreich and D. Turnbull (Academic, San Diego, 1989), Vol. 42, p 91.
[27] M. Sigrist, D. B. Bailey, and R. B. Laughlin, Phys. Rev. Lett. **74**, 3249 (1995).
[28] F. Tafuri, and J. R. Kirtley, preprint cond-mat/0003106.
[29] It is possible to treat this problem including inductive effects; see, for example, D. Dominguez, and J. V. Jose, Int. J. Mod. Phys. B **8**, 3749 (1994).
[30] A. Shapere, and F. Wilczek, *Geometric Phases in Physics,* (Singapore, Teaneck N.J., World Scientific Series, 1989).